IEEE Access
Multidisciplinary ⋮ Rapid Review ⋮ Open Access Journal

Received 12 December 2023, accepted 4 January 2024, date of publication 12 January 2024, date of current version 23 January 2024.

Digital Object Identifier 10.1109/ACCESS.2024.3353614

RESEARCH ARTICLE

Closed-Form Enhanced Detection of Clipped OFDM Symbol

ADRIANA LIPOVAC, ANTE MIHALJEVIĆ, AND VLATKO LIPOVAC
Department of Electrical Engineering and Computing, University of Dubrovnik, 20000 Dubrovnik, Croatia
Corresponding author: Adriana Lipovac (adriana.lipovac@unidu.hr)

ABSTRACT Large peak-to-average power ratio (PAPR) and carrier frequency offset (CFO) are dominant impairments of the orthogonal frequency-division multiplexing (OFDM) symbol transmission that is applied within the state-of-the-art wireless operator networks. In this work, we deal with consequences of the amplitude peak clipping that is commonly used at the transmitter to reduce the PAPR of the OFDM symbol, and thus prevent its non-linear distortion which would otherwise be imposed by the output high-power amplifier (HPA). Accordingly, regardless of the clipping generating mechanism at the transmitter being either inherent (related to the HPA) or deliberate (due to PAPR reduction), the clipped incoming OFDM symbol at the receiver may lead to degraded detection accuracy and transmission performance. However, the methods that have been applied so far at the receiver for compensating non-linear distortion due to clipping, are quite complex and computationally demanding. On the contrary, we propose effective mitigation of the problem to be performed at the receiver, by deriving the closed-form enhanced detection criterion, which requires common measurements of the mean and the rms values, as well as the autocorrelation of the received OFDM symbol comprising both un-clipped and clipped sections. Such improved detection was shown to significantly reduce the side effects of clipping, and restore satisfactory transmission performance – the bit error rate (BER) in particular. The proposed analytical model was preliminarily verified by versatile Monte-Carlo simulations and professional industry-standard vector signal analysis (VSA) test system, as well as by BER testing. The evident convergence of the three methods' test results leads to the conclusion that the proposed clipped OFDM symbol detection method provides clear improvement with respect to the conventional one.

INDEX TERMS OFDM, PAPR, clipping, distortion.

I. INTRODUCTION

Among the drawbacks of the orthogonal frequency-division multiplexing (OFDM) transmission over wireless channel, carrier frequency offset (CFO) and (large) peak-to-average power ratio (PAPR) dominantly degrade the transmission performance, and therefore require utmost attention in the state-of-the-art wireless networks of fourth and fifth generation - 4G and 5G, respectively, as well as with 6G to come in the foreseeable future [1], [2], [3].

With this regard, CFO hinders the carrier frequency synchronization between transmitter and receiver, which degrades mutual orthogonality of OFDM subcarriers, and thus causes inter-carrier interference (ICI) [2], [3], [4], [5]. On the other hand, when the overly high PAPR of the OFDM signal surpasses the dynamic range of the transmitter output high-power output amplifier (HPA), the latter is thus forced into saturation operating regime which causes clipping of peak signal values [6], [7], [8], [9], [10], [11], [12].

Various techniques have been proposed for CFO and high-PAPR mitigation [2], [3], [4], [5], [6], [7], [8], [9], [10], [11], [12], [13], which, for the latter, range from HPA linearization by inserting a digital pre-distorter (DPD) whose expansion characteristics is inverse to the compression one of the HPA [10], through neural network based approach [13],

The associate editor coordinating the review of this manuscript and approving it for publication was Yunlong Cai.

to peak amplitude clipping of the OFDM signal to be transmitted, as a simple and frequently applied method for PAPR reduction [9], [11].

With this regard, we have no goal here to deal with or provide any comparative analysis of various techniques for mitigating high PAPR at the transmitter. Rather, in the following, we focus the receiver, i.e. detection of the (time-wise) partially clipped OFDM symbol, regardless of the origin of clipping being either the transmitter HPA saturation, or the common PAPR reduction method applied at the transmitter to prevent the consequences of mismatching between (high) OFDM symbol dynamics (PAPR) and (limited) HPA linear operating regime zone.

As the clipped incoming OFDM symbol suffers from non-linear distortion and therefore degraded detection accuracy and transmission performance, some compensation of the negative effects of clipping may be applied at the receiver, such as maximum-likelihood based detection with iterative decoding [14], [15], whereas specifically the amplitude peaks are reconstructed in time domain [16], or the clipping noise is removed in frequency domain [17].

However, such methods for mitigating nonlinear effects of clipping are quite complex and therefore computationally demanding, even though that setback is to some extent diminished by more computation power available at the receiving base station than at the transmitting mobile one.

On the contrary, we propose effective mitigation of the high-PAPR effect at the receiver, by deriving the closed-form enhanced detection criterion, which requires quite simple measurements of the mean and the rms value, as well as of the autocorrelation of the received OFDM symbol being combined out of un-clipped and clipped sections.

Even though in the proposed OFDM detection model to follow, we justifiably consider the HPA non-linearity independent from the other channel or equipment impairments, let us note here that, out of the other major imperfections, time dispersion is very likely smaller than the OFDM symbol cyclic prefix (CP) which therefore reliably protects the OFDM symbol from inter-symbol interference (ISI) due to multipath propagation [18]. Thereby, under condition of large enough signal-to-noise ratio (SNR) and low CFO (e.g. residing after eventual compensation), this practically implies that the received symbol distortion due to clipping, solely determines detection accuracy, and thus the overall transmission performance.

This is where the main motivation for this work comes from, in order to find out how the standard OFDM detection can be enhanced to be less sensitive and vulnerable to peak clipping.

Following this goal, in Section II, the novel closed-form model for enhanced OFDM detection of the (partly) clipped signal is proposed, whereas the according test results are presented in Section III to verify the model. Conclusions are summarized in Section IV.

II. ANALYSIS

A. STANDARD OFDM DETECTION MODEL EXPLOITING THE ORTHOGONALITY OF SUBCARRIERS

The common OFDM transmission architecture is presented in Figure 1.

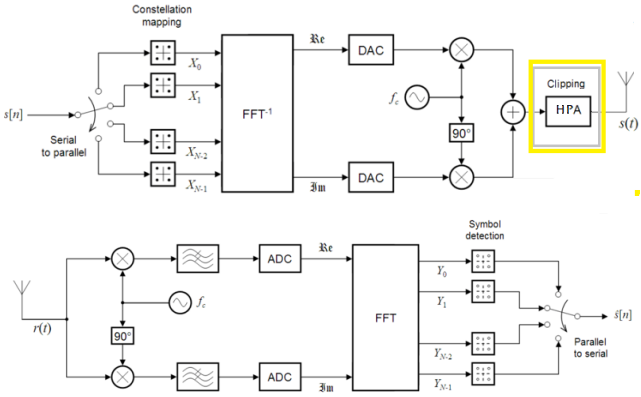

FIGURE 1. OFDM transmitter and receiver architecture with the transmitter HPA clipping the extensive-*PAPR*OFDM symbol.

Let us consider M OFDM sub-channels carrying T_s–long complex baseband symbols $\hat{s}_{m,n} = s_{m,n}e^{j\varphi_{m,n}}$; $m = 1, 2, \ldots, M$, which are summed to form the actually observed n-th transmitted composite OFDM symbol $\sum_{m=1}^{M} \hat{s}_{m,n} \cdot e^{\mathrm{j}m \cdot \frac{2\pi}{MT_s}\tau}$, where τ denotes the time-sampling delay [3].

If we assume distortion-free OFDM transmission, this implies that, at the receiver, a particular k-th original symbol $\hat{s}_{k,n} = s_{k,n}e^{j\varphi_{k,n}}$ can be detected within the incoming composite OFDM symbol $\sum_{m=1}^{M} \hat{r}_{k,n} \cdot e^{\mathrm{j}m \cdot \frac{2\pi}{MT_s}\tau}$ by exploiting the sub-carriers' orthogonality throughout the composite OFDM symbol time MT_s [18], in which case performing the orthogonality test with the k-th sub-carrier yields the following outcome:

$$\begin{aligned}\hat{r}_{k,n} &= \frac{1}{MT_s} \cdot \int_{(n-1)MT_s}^{nMT_s} \left(\sum_{m=1}^{M} \hat{s}_{m,n} \cdot e^{\mathrm{j}m \cdot \frac{2\pi}{MT_s}\tau} \right) \cdot e^{-\mathrm{j}k \cdot \frac{2\pi}{MT_s}\tau} d\tau \\ &= \frac{1}{MT_s} \cdot \sum_{m=1}^{M} \hat{s}_{m,n} \cdot \int_{(n-1)MT_s}^{nMT_s} e^{\mathrm{j}(m-k) \cdot \frac{2\pi}{MT_s}\tau} d\tau \\ &= \frac{1}{MT_s} \cdot \hat{s}_{k,n} \cdot \int_{0}^{MT_s} e^{\mathrm{j}(k-k) \cdot \frac{2\pi}{MT_s}\tau} d\tau \\ &= \hat{s}_{k,n} \end{aligned} \quad (1)$$

However, in practice, such an ideal scenario is not realistic, and therefore the perfect detection (1) is hindered by a number of above mentioned real-life impairments, out of which, we are to model and analyze the peak amplitude clipping of the OFDM symbol, as the consequence of pairing its large PAPR with the compressed dynamic range of the transmitter HPA, in particular.

B. MODELING DETECTION OF THE MIXED UNCLIPPED-CLIPPED OFDM SIGNAL

Consider the clipped OFDM symbol transmitted by the HPA with its mean power backed-off for the value *BACK-OFF* (expressed in decibels) from the saturation.

As it is visually justifiable by Figure 2, we speculate that, for higher *PAPR* and lower HPA *BACK-OFF*, we can expect more high-peak OFDM symbol "excursions" over the HPA saturation level, i.e. more clipping events.

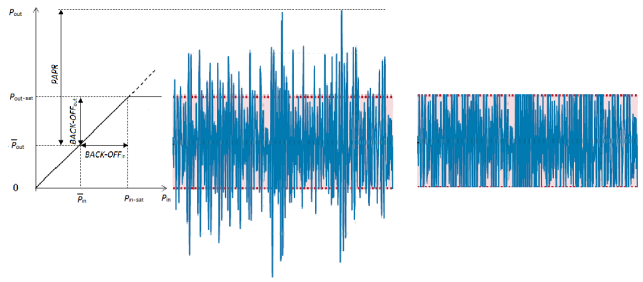

FIGURE 2. Transmitter HPA clipping the OFDM symbol.

When such (time-wise) partially clipped symbol arrives at the receiver input, the classical OFDM detection is applied on it. In that case, let us adopt that, out of the entire OFDM symbol duration MT_s, the summed unclipped parts take T_{UNCL} overall, whereas the summed clipped parts are $T_{CL} = MT_s - T_{UNCL}$ long in total.

Then again, the actual (k-th) sub-carrier is to be identified by applying the orthogonality test detection analogous to (1) modified to (2), as shown at the bottom of the next page, where in the integral limits we omitted (as irrelevant here) the OFDM symbols' sequence numbers "$n-1$" and "n", appearing in (1).

We solve the first left integral in (2) taking into account that its overall range $(0 - T_{UNCL})$ does not include the entire OFDM symbol interval MT_s but just the unclipped sections of it, so the unclipped-part detection in the k-th sub-channel of the received symbol, takes the following form:

$$\begin{aligned}\hat{r}_{k,n\_UNCL} &= \frac{1}{MT_s}\cdot\sum_{m=1}^{M}\hat{s}_{m,n}\cdot\int_{0}^{T_{UNCL}} e^{j(m-k)\cdot\frac{2\pi}{MT_s}\tau}d\tau \\ &= \frac{T_{UNCL}}{MT_s}\cdot\hat{s}_{k,n} + \sum_{\substack{m=1\\m\neq k}}^{M}\hat{s}_{m,n}\cdot\frac{e^{j(m-k)\cdot 2\pi\cdot\frac{T_{UNCL}}{MT_s}}-1}{j\,(m-k)\cdot 2\pi} \end{aligned} \quad (3)$$

Now let us solve the second (to the right) integral in (2) - the clipped-detection part of the received symbol in the k-th sub-channel, as it follows:

Having in mind that the signum function of a complex number $z = a + jb$ is defined as:

$$\mathrm{sgnz} = \frac{z}{|z|} = \frac{a+jb}{\sqrt{a^2+b^2}} \quad (4)$$

we apply (4) as it follows:

$$\hat{r}_{k,n\_CL} = \frac{1}{MT_s}\cdot\frac{\sum_{m=1}^{M}\hat{s}_{m,n}\cdot\int_{T_{UNCL}}^{MT_s} e^{j(m-k)\cdot\frac{2\pi}{MT_s}\tau}d\tau}{\left|\sum_{m=1}^{M}\hat{s}_{m,n}\cdot e^{jm\cdot\frac{2\pi}{MT_s}\tau}\right|} \quad (5)$$

where the denominator can be expressed as (6), shown at the bottom of the next page.

By substituting (6) into (5), the latter becomes:

$$\begin{aligned}\hat{r}_{k,n\_CL} = &\frac{\left(1-\frac{T_{UNCL}}{MT_s}\right)}{\sqrt{\sum_{i=1}^{M}\sum_{j=1}^{M}s_{i,n}s_{j,n}}}\cdot\hat{s}_{k,n} \\ &- \frac{\sum_{\substack{m=1\\m\neq k}}^{M}\hat{s}_{m,n}\cdot\frac{e^{j(m-k)\cdot 2\pi\cdot\frac{T_{UNCL}}{MT_s}}-1}{j(m-k)\cdot 2\pi}}{\sqrt{\sum_{i=1}^{M}\sum_{j=1}^{M}s_{i,n}s_{j,n}}}\end{aligned} \quad (7)$$

Furthermore, by substituting (3) and (7) into (2), we obtain:

$$\begin{aligned}\hat{r}_{k,n} = &\left(\frac{T_{UNCL}}{MT_s} + \frac{1-\frac{T_{UNCL}}{MT_s}}{\sqrt{\sum_{i=1}^{M}\sum_{j=1}^{M}s_{i,n}s_{j,n}}}\right)\cdot\hat{s}_{k,n} \\ &+ \sum_{\substack{m=1\\m\neq k}}^{M}\hat{s}_{m,n}\cdot\frac{e^{j(m-k)\cdot 2\pi\cdot\frac{T_{UNCL}}{MT_s}} - 1 - \frac{e^{j(m-k)\cdot 2\pi\cdot\frac{T_{UNCL}}{MT_s}}-1}{\sqrt{\sum_{i=1}^{M}\sum_{j=1}^{M}s_{i,n}s_{j,n}}}}{j\,(m-k)\cdot 2\pi}\end{aligned} \quad (8)$$

which we further simplify by developing the complex exponentials in series, and considering that it is their difference what matters here, which will not be much affected if only the two most significant terms are taken into account, so that (8) can be approximated as:

$$\begin{aligned}\hat{r}_{k,n} \approx &\left(\frac{T_{UNCL}}{MT_s} + \frac{1-\frac{T_{UNCL}}{MT_s}}{\sqrt{\sum_{i=1}^{M}\sum_{j=1}^{M}s_{i,n}s_{j,n}}}\right)\cdot\hat{s}_{k,n} \\ &+ \frac{T_{UNCL}}{MT_s}\cdot\left(1-\frac{1}{\sqrt{\sum_{i=1}^{M}\sum_{j=1}^{M}s_{i,n}s_{j,n}}}\right)\cdot\sum_{\substack{m=1\\m\neq k}}^{M}\hat{s}_{m,n}\end{aligned} \quad (9)$$

Let us recognize that, presuming mutually independent paired symbols $s_{i,n}, s_{j,n}$ of equal probabilities $1/M$ each to take any (k-th) value out of M possible ones, the double sum under the square root in (9) is proportional to the auto-correlation function R_{ss} of the transmitted unclipped n-th

composite OFDM symbol $\sum_{m=1}^{M} s_{m,n} e^{j\varphi_{m,n}} \cdot e^{\mathrm{j}m \cdot \frac{2\pi}{MT_\mathrm{s}}\tau}$, whose k-th distortion-less term $s_{k,n}e^{j\varphi_{k,n}} = \hat{s}_{k,n}$ is to be (ideally) received in the k-th sub-channel:

$$\begin{aligned} R_{ss} &= \sum_{i=1}^{M}\sum_{j=1}^{M} P\left(s_{i,n}, s_{j,n}\right) \cdot s_{i,n}s_{j,n} \\ &= \sum_{i=1}^{M}\sum_{j=1}^{M} P\left(s_{i,n}\right) \cdot P\left(s_{j,n}\right) \cdot s_{i,n}s_{j,n} \\ &= \frac{1}{M^2} \cdot \sum_{i=1}^{M}\sum_{j=1}^{M} s_{i,n}s_{j,n} \end{aligned} \tag{10}$$

Let us derive the autocorrelations also involving the clipped sections of the OFDM signal.

C. AUTOCORRELATION OF MIXED UNCLIPPED-CLIPPED OFDM SIGNAL

In our transmission scenario, any incoming (elementary) symbol $\hat{r}_{k,n}$; $k = 1, 2, \ldots, M$ within the overall OFDM symbol, can be received either ideally as $\hat{r}_{k,n} = \hat{s}_{k,n}$; $k = 1, 2, \ldots, M$, or as its clipped form $\hat{r}_{k,n} = \operatorname{sgn} \hat{s}_{k,n}$.

Thereby, at the receiver, the autocorrelation R_{ss} of the unclipped signal that is being transmitted, can be estimated from the autocorrelation R_{rr} of the received symbols – both the clipped and the unclipped ones, as it follows:

Once again considering the overall OFDM symbol time MT_s divided into the aggregated unclipped part T_UNCL and its clipped complement T_CL to MT_s (where the "aggregations" do not affect the generality of the model that we are developing here), the actual autocorrelation R_{rr} measured at the receiver is the average of the unclipped-only, the clipped-only and the mixed unclipped-clipped elementary-symbol products (11), as shown at the bottom of the next page.

As it comes out from (11), to estimate the autocorrelation R_{ss} from the received-signal combined unclipped-clipped-mixed autocorrelation R_{rr}, at first, we need to recognize that the first-left final-row term on the right side in (11) is already expressed by R_UNCL, but we also need to make it so with the remaining middle and right terms of (11), so to get its entire right side expressed by R_UNCL. This will determine the relationship between R_{rr}, estimated at the receiver, and R_UNCL, where the latter can be considered as the good enough approximation of R_{ss} for long enough T_UNCL(accentuating the wide-sense stationarity, of the autocorrelation in particular).

Following this plan, we proceed from our assumption that the OFDM symbol $\sum_{m=1}^{M} s_{m,n} e^{j\varphi_{m,n}} \cdot e^{\mathrm{j}m \cdot \frac{2\pi}{MT_\mathrm{s}}\tau}$, being the complex sum of enough many ($M \gg$) terms, can be justifiably regarded as the complex random variable with Gaussian distribution of the zero mean and the variance of $\sum_{m=1}^{M} s_{m,n}^2$. (This also applies to the baseband representation $\sum_{m=1}^{M} s_{m,n} e^{j\varphi_{m,n}}$). The Gaussian assumption enables applicability of the general relationship between the autocorrelation functions R_UNCL and R_CL of the Gaussian process and its hard-clipped version, respectively, onto the OFDM symbol, as it follows [19]:

$$R_\mathrm{CL} = \frac{2}{\pi} \cdot \sin^{-1} R_\mathrm{UNCL} \tag{12}$$

As it can be seen in (12) and the corresponding Figure 3, the analog signal autocorrelation takes larger values than the one of the hard-clipped signal, with the exception of their equality when both correlations approach zero or unity.

Now, when we expressed by (12) the utmost left term in (11) – the unclipped-OFDM-symbol autocorrelation, by the clipped-symbol one, let us do so for the middle term ($R_\mathrm{UNCL\text{-}CL}$), reasonably approximating it by the accordingly weighted value in between the unclipped and the clipped-signal autocorrelation:

$$R_\mathrm{CL} < R_\mathrm{UNCL\text{-}CL} < R_\mathrm{UNCL} \tag{13}$$

$$\begin{aligned} \hat{r}_{k,n} &= \frac{1}{MT_\mathrm{s}} \cdot \int_0^{T_\mathrm{UNCL}} \left(\sum_{m=1}^{M} \hat{s}_{m,n} \cdot e^{\mathrm{j}(m-k)\cdot\frac{2\pi}{MT_\mathrm{s}}\tau} \right) \cdot d\tau + \frac{1}{MT_\mathrm{s}} \cdot \int_{T_\mathrm{UNCL}}^{MT_\mathrm{s}} \operatorname{sgn}\left(\sum_{m=1}^{M} \hat{s}_{m,n} \cdot e^{\mathrm{j}(m-k)\cdot\frac{2\pi}{MT_\mathrm{s}}\tau} \right) \cdot d\tau \\ &= \frac{1}{MT_\mathrm{s}} \cdot \sum_{m=1}^{M} \hat{s}_{m,n} \cdot \int_0^{T_\mathrm{UNCL}} e^{\mathrm{j}(m-k)\cdot\frac{2\pi}{MT_\mathrm{s}}\tau} d\tau + \frac{1}{MT_\mathrm{s}} \cdot \int_{T_\mathrm{UNCL}}^{MT_\mathrm{s}} \operatorname{sgn}\left(\sum_{m=1}^{M} \hat{s}_{m,n} \cdot e^{\mathrm{j}(m-k)\cdot\frac{2\pi}{MT_\mathrm{s}}\tau} \right) \cdot d\tau \end{aligned} \tag{2}$$

$$\begin{aligned} \left| \sum_{m=1}^{M} \hat{s}_{m,n} \cdot e^{\mathrm{j}m\cdot\frac{2\pi}{MT_\mathrm{s}}\tau} \right| &= \left| \sum_{m=1}^{M} s_{m,n} \cos\left(\varphi_{m,n} + m \cdot \frac{2\pi}{MT_\mathrm{s}}\tau\right) + \mathrm{j} \sum_{m=1}^{M} s_{m,n} \sin\left(\varphi_{m,n} + m \cdot \frac{2\pi}{MT_\mathrm{s}}\tau\right) \right| \\ &= \sqrt{\sum_{i=1}^{M}\sum_{j=1}^{M} s_{i,n}s_{j,n}} \end{aligned} \tag{6}$$

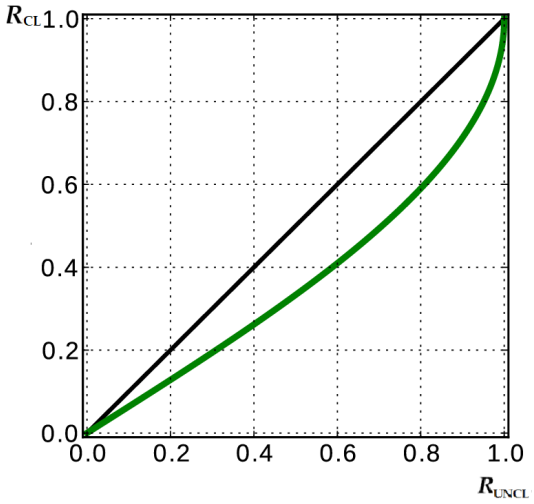

FIGURE 3. Relationship between the correlation function R_{UNCL} of the Gaussian random process and R_{CL} of its hard-clipped version.

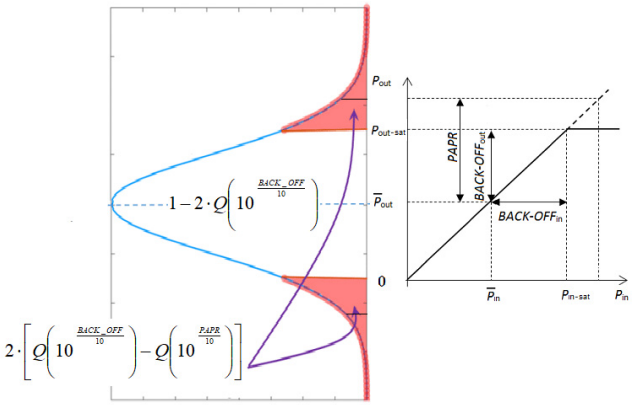

FIGURE 4. High-*PAPR* Gaussian-modeled OFDM symbol clipping by HPA.

Consequently, in that case, the "mixed" unclipped-clipped autocorrelation $R_{\mathrm{UNCL\text{-}CL}}$ gets closer to the clipped-clipped autocorrelation R_{CL}, and vice versa, which in turn implies appropriateness of the following estimation of the former one, where $Q(+)$ denotes the Gaussian distribution tail function):

$$R_{\mathrm{UNCL\text{-}CL}} \approx 2\cdot\left[\frac{1}{2}-Q\left(10^{\frac{BACK\_OFF}{10}}\right)\right]\cdot R_{\mathrm{UNCL}} + 2\cdot\left[Q\left(10^{\frac{BACK\_OFF}{10}}\right)-Q\left(10^{\frac{PAPR}{10}}\right)\right]\cdot R_{\mathrm{CL}} \tag{14}$$

As matter of fact, (14) is accordingly visualized in Figure 4, which is actually based on the "zoomed-in" left part of Figure 2. However, as OFDM symbol *PAPR* reaches quite high values, we consider the clipping event to occur each time the signal surpasses the *BACK-OFF* level, regardless of the actual *PAPR* value, specifically its difference with respect to the actual *BACK-OFF* value, which is the indicator of the OFDM symbol clipping potential.

Accordingly, we omit the far-right term in (14) that is anyway much smaller than its closest neighboring term to the left, and, by taking into account (12), as well as wide-sense stationarity (of autocorrelation, in this case), (14) reduces to:

$$R_{\mathrm{UNCL\text{-}CL}} \approx \left[1-2\cdot Q\left(10^{\frac{BACK\_OFF}{10}}\right)\right]\cdot R_{\mathrm{UNCL}} + 2\cdot Q\left(10^{\frac{BACK\_OFF}{10}}\right)\cdot\frac{2}{\pi}\cdot\sin^{-1}R_{\mathrm{UNCL}} \tag{15}$$

Moreover, for large total count of sub-carriers (M), justifiably considering the (OFDM symbol) correlation R_{ss} as well as R_{rr} to be quite small, we approximate the arc sine function with its argument adopting:

$$\sin^{-1}x = x+\frac{1}{6}\cdot x^3+\frac{3}{40}\cdot x^5+\ldots\approx x \tag{16}$$

which reduces (15) to:

$$R_{\mathrm{UNCL\text{-}CL}} \approx \left[1-\left(2-\frac{4}{\pi}\right)\cdot Q\left(10^{\frac{BACK\_OFF}{10}}\right)\right]\cdot R_{\mathrm{UNCL}} \tag{17}$$

Now, in order to get the autocorrelation R_{rr} at the receiver, let us first modify (11) by substituting (12) and (17) in it, before taking into account that, analogously to the earlier defined and used ratio $\frac{T_{\mathrm{UNCL}}}{MT_s}$, the count M_{UNCL} of un-clipped elementary symbols relative to their total count M within the observed (n-th) composite OFDM symbol, is monotonic with *BACK-OFF*:

$$\frac{M_{\mathrm{UNCL}}}{M} \approx 1-2\cdot Q\left(10^{\frac{BACK\_OFF}{10}}\right) \tag{18}$$

$$\begin{aligned} R_{rr} &= \frac{1}{M^2}\cdot\sum_{i=1}^{M}\sum_{j=1}^{M} r_{i,n}r_{j,n} \\ &= \frac{1}{M^2}\cdot\left(\sum_{i=1}^{M_{\mathrm{UNCL}}}\sum_{j=1}^{M_{\mathrm{UNCL}}} s_{i,n}s_{j,n}+\sum_{i=1}^{M_{\mathrm{UNCL}}}\sum_{j=M_{\mathrm{UNCL}}+1}^{M} s_{i,n}\cdot\operatorname{sgn}s_{j,n}+\sum_{i=M_{\mathrm{UNCL}}+1}^{M}\sum_{j=M_{\mathrm{UNCL}}+1}^{M}\operatorname{sgn}s_{i,n}\cdot\operatorname{sgn}s_{j,n}\right) \\ &\approx \frac{M_{\mathrm{UNCL}}^2}{M^2}\cdot R_{\mathrm{UNCL}}+\frac{M_{\mathrm{UNCL}}\cdot\left(M-M_{\mathrm{UNCL}}\right)}{M^2}\cdot R_{\mathrm{UNCL\text{-}CL}}+\frac{\left(M-M_{\mathrm{UNCL}}\right)^2}{M^2}\cdot R_{\mathrm{CL}} \end{aligned} \tag{11}$$

which is also substituted into (11), so that we obtain (19), as shown at the bottom of the page, where, having in mind $Q(\cdot)$ function fast decay, we can confidently omit the (very) smallest last term comprising $Q^3(\cdot)$, whereas we were initially concerned to neglect the middle term containing $Q^2(\cdot)$ as well, specifically for the smaller *BACK-OFF* values. With this regard, let us note that, from (19), it is evident that omitting $Q^2(\cdot)$ decreases the square root (monotonic with R_{rr}) in both denominators in (9), thus increasing the left term (scaled ideal signal), while reducing the right one (interference), which at least keeps the "balance" of (9), not to mention the (unexpected) detection benefit. In addition, we were further encouraged by the related specific MC simulations, to finally reduce (19) to:

$$R_{rr} = \frac{1}{M^2}\cdot\sum_{i=1}^{M}\sum_{j=1}^{M} r_{i,n}r_{j,n} \approx \left[1-2\cdot Q\left(10^{\frac{BACK\_OFF}{10}}\right)\right]\cdot R_{z}^{\mathrm{UNCL}} \tag{20}$$

Furthermore, coming out of (20), simple relation between the targeted (in (9)/(10)) distortionless-symbol autocorrelation R_{ss} (close to the one of the unclipped symbol section: $R_{ss}\approx R_{\mathrm{UNCL}}$) and the actual (i.e. measurable at the receiver) autocorrelation R_{rr}:

$$R_{ss} \approx \frac{R_{rr}}{1-2\cdot Q\left(10^{\frac{BACK\_OFF}{10}}\right)} \tag{21}$$

implies that, finally, the following substitution with this regard is to be inserted in (9):

$$\sqrt{\sum_{i=1}^{M}\sum_{j=1}^{M} s_{i,n}s_{j,n}} = M\cdot\sqrt{\frac{R_{rr}}{1-2\cdot Q\left(10^{\frac{BACK\_OFF}{10}}\right)}} \tag{22}$$

But before that, let us consider how we can estimate the remaining sum $\sum_{\substack{m=1\\m\neq k}}^{M}\hat{s}_{m,n}$ of the undistorted received symbols, which is also needed in (9), as it expresses the intersymbol interference out of all other elementary symbols (within the observed (n-th) composite OFDM symbol) onto the k-th one being detected.

D. AVERAGE OF MIXED UNCLIPPED–CLIPPED OFDM SIGNAL

Let us apply a similar (but somewhat simpler) approach that we used above to estimate the non-clipped signal autocorrelation R_{ss} from the actual autocorrelation R_{rr} measurable at the receiver. So, at this time, we again recall the wide-sense stationarity of not only autocorrelation, but also of the received symbol mean value and mean power, to estimate the cumulative sum (needed in (9)) $S_s = \sum_{\substack{m=1\\m\neq k}}^{M}\hat{s}_{m,n}$ of the unclipped transmitted elementary symbols (constituting the actual composite OFDM symbol) from the corresponding sum S_r of all received - clipped and clipped symbols (except the k-th one), which, analogously with (4), (6) and (11), we estimate as (23), shown at the bottom of the next page, where P_{CL} is the overall power corresponding to the (later) clipped section of the transmitted OFDM symbol, whereas $E\left[\hat{s}_{m,n,\mathrm{UNCL}}\right]$ and $E\left[\hat{s}_{m,n,\mathrm{CL}}\right]$ are the average values of the symbols belonging to the un-clipped and the (later) clipped OFDM symbol sections, respectively. As the sum S_r determines the corresponding mean $E\left[\hat{r}_{m,n}\right]$ of the received symbol, we rephrase (23) in terms of the other two relevant mean values, also taking into account (18), to obtain:

$$E\left[\hat{r}_{m,n}\right] = \frac{S_r}{M} \approx \left[1-2\cdot Q\left(10^{\frac{BACK\_OFF}{10}}\right)\right]\cdot E\left[\hat{s}_{m,n,\mathrm{UNCL}}\right] + 2\cdot Q\left(10^{\frac{BACK\_OFF}{10}}\right)\cdot\frac{E\left[\hat{s}_{m,n,\mathrm{CL}}\right]}{\sqrt{P_{\mathrm{CL}}}} \tag{24}$$

Since, generally, the mean power P_{CL} of the OFDM symbol clipped section equals the zero-time-leg autocorrelation, (15) and (16) apply here as well (but at this time, we express P_{UNCL} by P_{CL}), so the OFDM symbol mean power $E\left[r_{m,n}^2\right]$ at the receiver is:

$$E\left[r_{m,n}^2\right] \approx \left\{\frac{\pi}{2}\cdot\left[1-2\cdot Q\left(10^{\frac{BACK\_OFF}{10}}\right)\right] + 2\cdot Q\left(10^{\frac{BACK\_OFF}{10}}\right)\right\}\cdot P_{\mathrm{CL}} \tag{25}$$

$$\begin{aligned} R_{rr} &= \frac{1}{M^2}\cdot\sum_{i=1}^{M}\sum_{j=1}^{M} r_{i,n}r_{j,n} \\ &\approx \left\{\left[1-2\cdot Q\left(10^{\frac{BACK\_OFF}{10}}\right)\right]^2 + \left[1-2\cdot Q\left(10^{\frac{BACK\_OFF}{10}}\right)\right]\cdot 2\cdot Q\left(10^{\frac{BACK\_OFF}{10}}\right)\right. \\ &\quad \left.\cdot\left[1-\left(2-\frac{4}{\pi}\right)\cdot Q\left(10^{\frac{BACK\_OFF}{10}}\right)\right] + \frac{8}{\pi}\cdot Q^2\left(10^{\frac{BACK\_OFF}{10}}\right)\right\}\cdot R_{\mathrm{UNCL}} \\ &\approx \left\{1-2\cdot Q\left(10^{\frac{BACK\_OFF}{10}}\right) + \left(\frac{16}{\pi}-4\right)\cdot Q^2\left(10^{\frac{BACK\_OFF}{10}}\right) + \left(8-\frac{16}{\pi}\right)\cdot Q^3\left(10^{\frac{BACK\_OFF}{10}}\right)\right\}\cdot R_{z}^{\mathrm{UNCL}} \end{aligned} \tag{19}$$

From (25), it follows that:

$$P_{\mathrm{CL}} \approx \frac{E\left[r_{m,n}^2\right]}{\frac{\pi}{2}\cdot\left[1-2\cdot Q\left(10^{\frac{BACK\_OFF}{10}}\right)\right]+2\cdot Q\left(10^{\frac{BACK\_OFF}{10}}\right)} \tag{26}$$

which we substitute into (24) to obtain the following expected value of the received symbol (27), as shown at the bottom of the next page.

Here again we can reasonably assume that, for enough many OFDM subcarriers, i.e. for large enough M(and so M_{UNCL} and M_{CL} alike) highlighting the wide-sense stationarity, the means $E\left[\hat{s}_{m,n,\mathrm{UNCL}}\right]$ and $E\left[\hat{s}_{m,n,\mathrm{CL}}\right]$ corresponding to the un-clipped and to the clipped sections, respectively, are quite close one to each other and to the overall OFDM symbol mean $E\left[\hat{s}_{m,n}\right]$, so (27) can take the following form (28), as shown at the bottom of the next page.

Finally, (28) implies that (29), as shown at the bottom of the next page.

Now when we have found the last term – the utmost right one in (9), by taking into account (18), (22) and (29), (9) is finally transformed to the following detection outcome (30), as shown at the bottom of the next page.

As it is evident from (30), the received k-th elementary symbol $\hat{r}_{k,n}$ (comprised by the n-th composite OFDM symbol being clipped by the HPA at the transmitter) consists of the scaled undistorted symbol $\hat{s}_{k,n}$ and the interference term. Accordingly, the proposed enhanced detection (30) firstly requires estimating the right-side additive term to subtract it from the received symbol $\hat{r}_{k,n}$, and then divide the obtained result by the ''coefficient'' in front of $\hat{s}_{k,n}$. Precedingly, the autocorrelation R_{rr}, the mean power $E\left[r_{m,n}^2\right]$ and the mean $E\left[\hat{r}_{m,n}\right]$ of the received (mixed un-clipped and clipped) OFDM symbol, need to be measured.

E. ACCURACY OF THE ENHANCED SYMBOL DETECTION

The residual inaccuracy of the proposed enhanced detection by means of (30) is determined by the rms distortion of the so detected received OFDM symbol with respect to the distortion-free one, i.e. by the data-averaged error vector magnitude (EVM) [20]:

$$EVM = \sqrt{\mathrm{E}\left[\frac{s_{k,n}^2 - r_{k,n}^2}{s_{k,n}^2}\right]} = \sqrt{\sum_{k=1}^{M}\frac{s_{k,n}^2 - r_{k,n}^2}{s_{k,n}^2}} \tag{31}$$

Although, generally, measuring EVM as a comprehensive single-number radio link health indicator providing insight into the modulation symbols' susceptibility (not only to noise, but also to other impairments being neither additive nor linear), bears a clear added value with respect to pure bit error rate (BER) testing [16], still we consider the two methods significantly complementary one to each other, and therefore BER testing worth of including into the verification of (30), in addition to EVM measurements.

With this purpose, in case of no standalone transmission performance test device available, we can estimate the HPA-distortion-caused BER by recalling its monotonic functional relationship with EVM, which applies for the M_{QAM}-ary QAM as it follows [21] and [22]:

$$BER = \frac{4}{\log_2 M_{\mathrm{QAM}}}\cdot Q\left(\sqrt{\frac{3}{EVM^2\cdot\left(M_{\mathrm{QAM}}-1\right)}}\right) \tag{32}$$

III. TEST RESULTS

A. OFDM DETECTION TEST SYSTEM SETUP

We implemented the common OFDM transmission architecture presented in Figure 1, by means of MATLAB simulation tools, where we adopted 256 subcarriers with 16 QAM modulation, and, specifically, the mean transmitter power of 0 dBm (with no loss of generality, though the mobile station and the base station power means of less than 1% out of 23 dBm or 42 dBm maximal output power, respectively, can be expected e.g. in 4G/5G networks [4]).

Analogously to the schematic in Figure 1, in our test system presented in Figure 5, we added the ''clipping'' determinant to the transmitter output HPA block, whereas the detection at the receiver remained the same as with the conventional OFDM receiver, but with the additional estimations of the mean, the rms value and the autocorrelation needed for the enhanced detection (30). Moreover, the lower-right block

$$\begin{aligned} S_r &= \sum_{\substack{m=1\\ m\neq k}}^{M}\hat{r}_{m,n} \\ &= \sum_{\substack{m=1\\ m\neq k}}^{M_{\mathrm{UNCL}}}\hat{s}_{m,n} + \mathrm{sgn}\sum_{\substack{m=M_{\mathrm{UNCL}}+1\\ m\neq k}}^{M}\hat{s}_{m,n} \\ &\approx M\cdot\frac{M_{\mathrm{UNCL}}}{M}\cdot E\left[\hat{s}_{m,n,\mathrm{UNCL}}\right] + M\cdot\left(1-\frac{M_{\mathrm{UNCL}}}{M}\right)\cdot\frac{E\left[\hat{s}_{m,n,\mathrm{CL}}\right]}{\sqrt{P_{\mathrm{CL}}}}; \quad P_{\mathrm{CL}} = \sum_{\substack{m=M_{\mathrm{UNCL}}+1\\ m\neq k}}^{M}s_{m,n}^2 \end{aligned} \tag{23}$$

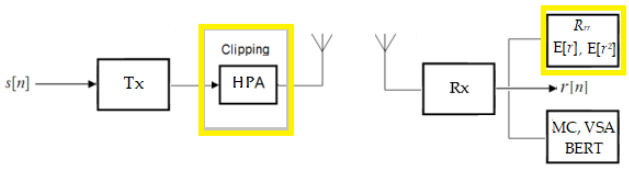

FIGURE 5. Test system block-schematic; the yellow frame highlights clipping at the transmitter and the related processing at the receiver (without the indices *m*, *n* in the mean and rms values of the received signal). The tests include MC simulations, VSA and BERT.

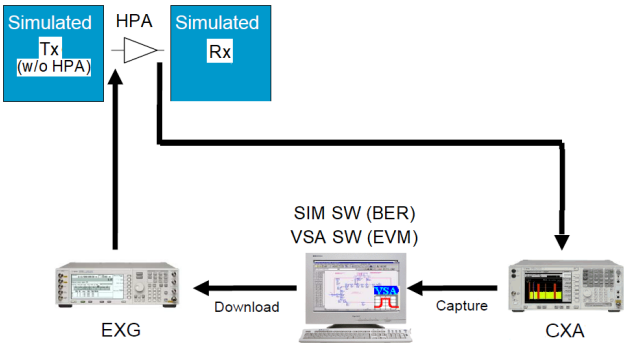

FIGURE 6. VSA based *EVM* and *BER* testing; EXG and CXA denote the specific VSG and VSA receiver, respectively.

comprises the detection model verification test tools: Monte Carlo (MC) simulations, vector signal analysis (VSA) and BER testing (BERT).

The channel was considered practically multipath-free and CFO-free, owing to supposedly long enough CP and successful CFO compensation, respectively. This enables focusing our tests onto the peak clipping effects exclusively.

We tested EVM by MC simulations with or without the enhanced detection (30) applied, and complemented them with the industrial R&D-level VSA testing, in order to strengthen the verification of (30) by means of the special hardware - vector signal generator (VSG) and vector signal analyzer (VSA), and the related professional VSA software [23], [24], which we set up in our digital radio test lab, according to the HW/SW schematic presented in Figure 6.

Such an approach is common in the industry, as it allows testing of a developed transmitter or receiver component or sub-assembly, while simultaneously simulating their interoperating environment by VSA hardware and software (with

$$E\left[\hat{r}_{m,n}\right] \approx \left[1-2\cdot Q\left(10^{\frac{B_{ACK,OFF}}{10}}\right)\right]\cdot E\left[\hat{s}_{m,n,\mathrm{UNCI}}\right]+2\cdot Q\left(10^{\frac{BACK\_OFF}{10}}\right)\cdot \frac{E\left[\hat{s}_{m,n,\mathrm{CL}}\right]}{\sqrt{\frac{E\left[r_{m,n}^2\right]}{\frac{\pi}{2}\cdot\left[1-2\cdot Q\left(10^{\frac{BACK\_OFF}{10}}\right)\right]+2\cdot Q\left(10^{\frac{BACK\_OFF}{10}}\right)}}\,s} \tag{27}$$

$$E\left[\hat{r}_{m,n}\right] \approx \left\{\left[1-2\cdot Q\left(10^{\frac{BACK\_OFF}{10}}\right)\right]+2\cdot Q\left(10^{\frac{BACK\_OFF}{10}}\right)\cdot \frac{1}{\sqrt{\frac{E\left[r_{m,n}^2\right]}{\frac{\pi}{2}\cdot\left[1-2\cdot Q\left(10^{\frac{BACK\_OFF}{10}}\right)\right]+2\cdot Q\left(10^{\frac{BACK\_OFF}{10}}\right)}}}\right\}\cdot E\left[\hat{s}_{m,n}\right] \tag{28}$$

$$\sum_{\substack{m=1\\ m\neq k}}^{M}\hat{s}_{m,n} = \frac{M\cdot E\left[\hat{r}_{m,n}\right]}{\left[1-2\cdot Q\left(10^{\frac{BACK\_OFF}{10}}\right)\right]+\frac{2\cdot Q\left(10^{\frac{BACK\_OFF}{10}}\right)}{\sqrt{\frac{E\left[r_{m,n}^2\right]}{\frac{\pi}{2}\cdot\left[1-2\cdot Q\left(10^{\frac{BACK\_OFF}{10}}\right)\right]+2\cdot Q\left(10^{\frac{BACK\_OFF}{10}}\right)}}}} \tag{29}$$

$$\hat{r}_{k,n} \approx \left\{C_Q+\frac{1-C_Q}{M\cdot\sqrt{\frac{R_{rr}}{C_Q}}}\right\}\cdot\hat{s}_{k,n}+C_Q\cdot\left(1-\frac{1}{M\cdot\sqrt{\frac{R_{rr}}{C_Q}}}\right)\cdot\frac{M\cdot E\left[\hat{r}_{m,n}\right]}{C_Q+\frac{1-C_Q}{\sqrt{\frac{E\left[r_{m,n}^2\right]}{1+\left(\frac{\pi}{2}-1\right)\cdot C_Q}}}}$$

$$C_Q\left(BACK\_OFF\right) = 1-2Q\left(10^{\frac{BACK\_OFF}{10}}\right) \tag{30}$$

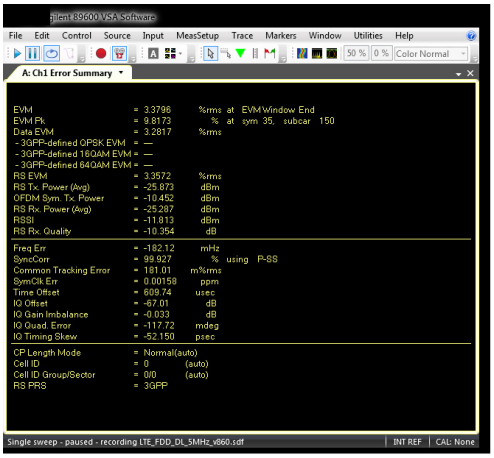

FIGURE 7. VSA Error Summary report screen shot with the *EVM* percentage (mapped into the corresponding entry in Table 1).

MATLAB API). This relaxes the need for simultaneous availability of the other system parts, interfacing the component under verification testing.

The VSA software was used as the industrial-level flexible tool to create various signal waveforms (OFDM in particular) to be downloaded to the VSG and thus drive the HPA under test, for which we chose the microwave preamplifier at hand - HP 8449B [25] (earlier primarily aimed as an external front-end for the older-generation spectrum analyzers). The HPA response was captured by the VSA receiver to forward it to the VSA SW for post-processing. (With somewhat less comfort, the *EVM* values could also be read directly from the VSA receiver display.)

B. TEST RESULTS

As it is already mentioned above, the test results are centered around the data-averaged clipping-caused *EVM* obtained from MC simulations, with or without the detection (30) applied, as well as from the VSA Error Summary reports, such as the exemplar one presented in the screen-shot in Figure 7, showing the average *EVM* value of 3.28% which corresponds to the *BACK-OFF* value of 9 dB.

Accordingly, in the following Table 1, as well as in the related bar chart in Figure 8, we firstly present the values of the relevant parameters - the OFDM *PAPR* and HPA *BACK-OFF* in particular, followed by their complementary cumulative distribution function (CCDF) values. Then, the MC-estimated (30)-based residual *EVM* values are listed for the three chosen *BACK-OFF* values, followed by the MC-estimated and VSA-tested ones with no detection enhancement applied. Finally, we compare the BERT results estimated by (32) for the (30)-based symbol detection, with the corresponding ones coming out of the MC simulations and VSA tests, both with no improved detection applied.

As it can be seen from the entries in Table 1, and the corresponding bar chart in Figure 8, we clarify that, generally, introducing the enhanced detection (30) significantly reduces the rms *EVM* - i.e. the average OFDM symbol distortion (31),

TABLE 1. Detection accuracy key indicators for the mixed unclipped-clipped OFDM symbol: residual rms distortion – *EVM* (%) and *BER* - MC-simulated ((30)-based or not), and VSA-based.

PAPR [dB]	5 (3.16 mW)	8 (6.31 mW)	11 (12.59 mW)
CCDF (*PAPR*)	0.36	0.08	$3.4{\cdot}10^{-4}$
BACK-OFF [dB]	3 (2 mW)	6 (4 mW)	9 (8 mW)
CCDF (*BACK-OFF*)	0.51	0.26	0.03
$EVM_{(30)}$%	2.48	2.37	2.25
$EVM_{(MC)}$%	4.62	3.82	3.20
$EVM_{(VSA)}$%	4.81	3.98	3.28
BER_{UNCL}	0	0	0
$BER_{(30)}$	$4.94{\cdot}10^{-7}$	$4.61{\cdot}10^{-7}$	$4.34{\cdot}10^{-7}$
$BER_{(MC)}$	$6.23{\cdot}10^{-4}$	$1.29{\cdot}10^{-5}$	$2.67{\cdot}10^{-6}$
$BER_{(VSA)}$	$8.56{\cdot}10^{-4}$	$2.34{\cdot}10^{-5}$	$2.84{\cdot}10^{-6}$

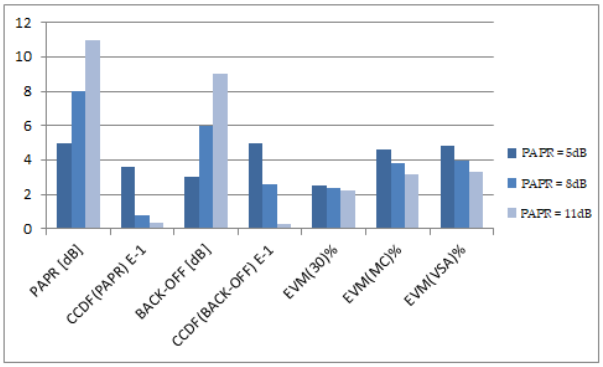

FIGURE 8. Data-averaged *EVM* of the partially clipped OFDM symbol, estimated by the MC simulations (with and w/o the enhanced detection (30)) and by the VSA tests, with the indexes „30", „MC" and „VSA", respectively, corresponding to the mapped entries in Table 1.

with respect to the case of no enhancement applied, when only increasing the *BACK-OFF* and consequent lowering its CCDF (in Section II considered as the Gaussian Q-tail function) is shown to prevent the HPA-caused distortion.

Such an *EVM* values trend is found to be accordingly (i.e. monotonically) tracked by the *BER* values in Table 1 and Figure 9, being ideally zeros with no transmitter HPA clipping (and supposed no other channel or equipment impairment), followed by the clipping-caused *BER* values, firstly estimated by the enhanced detection (30) and then by the evidently larger ones coming out of the MC simulations. Moreover, the VSA-provided *EVM* and the corresponding BERT estimated by (32), though set up to conform as much as possible to the MC running conditions, inevitably picked up various inherent residual real-life impairments, which is why the according VSA-based *BER* values are somewhat higher than the MC-generated ones, and thus present the practical upper-bound reference in this case.

Finally, in both Table 1 and Figures 8 and 9, it is obvious that extending the *BACK-OFF* (i.e. the HPA linear operating regime zone) improves the (30)-based *EVM* and *BER* values, but very slowly, whereas it is not so without applying (30) in MC tests, as well as in the VSA-based ones, when both *EVM* and *BER* values exhibit much more dispersion with the increasing *BACK-OFF*.

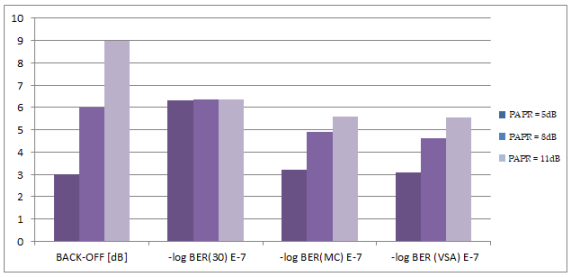

FIGURE 9. ***BER*** **of the partially clipped OFDM symbol, estimated by the MC simulations (with and w/o the enhanced detection (30)), and by the VSA tests, with the indexes „30", „MC" and „VSA", respectively, corresponding to the mapped entries in Table 1.**

So, based on both observation levels – the OFDM symbol rms distortion (*EVM*) and, the *BER*, it comes out that the benefits of the proposed enhanced detection of the mixed un-clipped and clipped symbol sections, are thus verified.

At this point, let us note that the purpose of the preliminary test results is only a very basic verification of the proposed concept, whereas various resources-rich and more versatile industrial-type follow-up tests, also taking into account other influencing factors under diverse practical conditions, are planned for the next phase of this research.

IV. CONCLUSION

Amplitude peak clipping is a common simple method for preventing the high-PAPR OFDM symbol from being non-linearly distorted by the transmitter HPA operating in saturation regime that would otherwise hinder OFDM detection at the receiver.

However, detecting the clipped incoming signal at the receiver presents a challenge of its own, but instead of computationally intensive methods that have been used so far for mitigation of the non-linear distortion due to clipping, we derive a simple closed-form improvement of the standard OFDM receiver detection, accommodating it to the (time-wise) partially clipped received OFDM symbol, by the according pre-detection processing involving the mean and the rms value, as well as the autocorrelation of the received OFDM symbol.

The preliminary verification of the proposed analytical model included not only the utmost versatile MC simulations, but also the professional industry-standard VSA and BER testing. The according test results coming out of all three test levels, were found mutually compliant, as for the proposed improved detection, the evident drop of the rms symbol distortion was monotonically followed by the lower corresponding BER values, as compared to the respective values achieved by the standard detection.

This finally presents the plain benefit of the proposed enhanced detection of the partially clipped OFDM symbol, with respect to the conventional detection.

REFERENCES

[1] D. Dardari, V. Tralli, and A. Vaccari, "A theoretical characterization of nonlinear distortion effects in OFDM systems," *IEEE Trans. Commun.*, vol. 48, no. 10, pp. 1755–1764, Oct. 2000.

[2] A. Lipovac and A. Mihaljevic, "In-service BER based estimation of OFDM PAPR and CFO-induced peak phase deviation," *J. Commun. Softw. Syst.*, vol. 15, no. 1, pp. 44–51, 2019.

[3] A. Lipovac, V. Lipovac, and P. Njemčević, "Suppressing the OFDM CFO-caused constellation symbol phase deviation by PAPR reduction," *Wireless Commun. Mobile Comput.*, vol. 2018, pp. 1–8, Aug. 2018.

[4] A. Mihaljević, A. Lipovac, V. Lipovac, and J. Musovic, "Practical BER-based estimation of residual OFDM CFO by reducing noise margin," *Wireless Commun. Mobile Comput.*, vol. 2020, pp. 1–5, Sep. 2020.

[5] H. Abdzadeh-Ziabari, W.-P. Zhu, and M. N. S. Swamy, "Joint maximum likelihood timing, frequency offset, and doubly selective channel estimation for OFDM systems," *IEEE Trans. Veh. Technol.*, vol. 67, no. 3, pp. 2787–2791, Mar. 2018.

[6] T. Jiang and Y. Wu, "An overview: Peak-to-average power ratio reduction techniques for OFDM signals," *IEEE Trans. Broadcast.*, vol. 54, no. 2, pp. 257–268, Jun. 2008.

[7] D.-F. Tseng, Y. S. Han, W. H. Mow, L.-C. Chang, and A. J. H. Vinck, "Robust clipping for OFDM transmissions over memoryless impulsive noise channels," *IEEE Commun. Lett.*, vol. 16, no. 7, pp. 1110–1113, Jul. 2012.

[8] S. Hee Han and J. Hong Lee, "Modulation, coding and signal processing for wireless communications—An overview of peak-to-average power ratio reduction techniques for multicarrier transmission," *IEEE Wireless Commun.*, vol. 12, no. 2, pp. 56–65, Apr. 2005.

[9] D. Guel and J. Palicot, "Analysis and comparison of clipping techniques for OFDM Peak-to-Average power ratio reduction," *IEEE Trans. Broadcast.*, vol. 53, no. 3, pp. 719–724, Jul. 2007.

[10] A. N. D'Andrea, V. Lottici, and R. Reggiannini, "RF power amplifier linearization through amplitude and phase predistortion," *IEEE Trans. Commun.*, vol. 44, no. 11, pp. 1477–1484, Nov. 1996, doi: 10.1109/26.544464.

[11] H. Ochiai and H. Imai, "Performance analysis of deliberately clipped OFDM signals," *IEEE Trans. Commun.*, vol. 50, no. 1, pp. 89–101, Jan. 2002.

[12] C. He and J. Armstrong, "Clipping noise mitigation in optical OFDM systems," *IEEE Commun. Lett.*, vol. 21, no. 3, pp. 548–551, Mar. 2017.

[13] I. Sohn, "A low complexity PAPR reduction scheme for OFDM systems via neural networks," *IEEE Commun. Lett.*, vol. 18, no. 2, pp. 225–228, Feb. 2014, doi: 10.1109/LCOMM.2013.123113.131888.

[14] J. Tellado-Mourelo, L. Hoo, and J. M. Cioffi, "Maximum likelihood detection of nonlinearly distorted multicarrier symbols by iterative decoding," *IEEE Trans. Commun.*, vol. 51, no. 2, pp. 218–228, Feb. 2003.

[15] F. H. Gregorio, S. Werner, J. Cousseau, J. Figueroa, and R. Wichman, "Receiver-side nonlinearities mitigation using an extended iterative decision-based technique," *Signal Process.*, vol. 91, no. 8, pp. 2042–2056, Aug. 2011.

[16] N. Bibi, A. Kleerekoper, N. Muhammad, and B. Cheetham, "Equation-method for correcting clipping errors in OFDM signals," *SpringerPlus*, vol. 5, no. 1, p. 931, Dec. 2016, doi: 10.1186/s40064-016-2413-0.

[17] H. Chen and A. Haimovich, "An iterative method to restore the performance of clipped and filtered OFDM signals," in *Proc. IEEE Int. Conf. Commun. (ICC)*, Anchorage, USA, May 2003, pp. 3438–3442, doi: 10.1109/ICC.2003.1204093.

[18] A. Lipovac, V. Lipovac, and B. Modlic, "PHY, MAC, and RLC layer based estimation of optimal cyclic prefix length," *Sensors*, vol. 21, no. 14, p. 4796, Jul. 2021, doi: 10.3390/s21144796.

[19] J. H. Van Vleck and D. Middleton, "The spectrum of clipped noise," *Proc. IEEE*, vol. 54, no. 1, pp. 2–19, Jan. 1966, doi: 10.1109/PROC.1966.4567.

[20] M. Rumnay, *LTE and the Evolution of 4G Wireless; Design and Measurements Challenges*, 2nd ed. Hoboken, NJ, USA: Wiley, 2013.

[21] H. A. Mahmoud and H. Arslan, "Error vector magnitude to SNR conversion for nondata-aided receivers," *IEEE Trans. Wireless Commun.*, vol. 8, no. 5, pp. 2694–2704, May 2009.

[22] A. Lipovac, B. Modlic, and M. Grgic, "OFDM error floor based EVM estimation," in *Proc. 24th Int. Conf. Softw., Telecommun. Comput. Netw. (SoftCOM)*, Sep. 2016, pp. 1–5.

[23] *3GPP LTE Modulation Analysis 89600 Vector Signal Analysis Software*, Agilent Technologies, Maharashtra, India, 2010.

[24] *Hardware Measurement Platforms for the Agilent 89600 Series Vector Signal Analysis Software*, document 5989-1753EN, Agilent Technologies, 2011.

[25] *Hewlett-Packard, HP 8449B; 1 to 26.5 GHz Preamplifier*, Operation and Service Manual, Hewlett Packard, 1990.